Vol. **111** (2007) *ACTA PHYSICA POLONICA A* No. 5

Proceedings of the XII National School "Correlated Electron Systems...", Ustroń 2006

The Existence of the 60 K Plateau in the $YBa_2Cu_3O_{6+y}$ Phase Diagram: the Role of Oxygen Ordering and Charge Imbalance

T.A. Zaleski and T.K. Kopeć

Institute of Low Temperature and Structure Research
Polish Academy of Sciences, P.O. Box 1410, 50-950 Wrocław, Poland

We propose a semi-microscopic model of $YBa_2Cu_3O_{6+y}$ to investigate the origin of the 60 K plateau in its phase diagram. Our model is a "phase only" approach to the high-temperature superconducting system in terms of collective variables. It is able to capture characteristic energy scales present in $YBa_2Cu_3O_{6+y}$ by using adjustable parameters representing phase stiffnesses and allows for strong anisotropy within basal planes to simulate oxygen ordering. We solve the model calculated T_c for chosen system parameters investigating the influence of oxygen ordering and doping imbalance on the shape of $YBa_2Cu_3O_{6+y}$ phase diagram. Our results suggest that the oxygen ordering alone does not seem to be responsible for the existence of the 60 K plateau. However, relying on experimental data unveiling that oxygen doping of $YBa_2Cu_3O_{6+y}$ may introduce a significant charge imbalance between CuO_2 planes and other sites, we show that *simultaneously* the former are underdoped, while the latter — strongly overdoped almost in the whole region of oxygen doping in which $YBa_2Cu_3O_{6+y}$ is superconducting. This provides two natural counter acting factors, which possibly lead to rise the 60 K plateau with increasing oxygen doping.

PACS numbers: 74.20.–z, 74.72.Bk, 74.62.–c

1. Introduction

The $YBa_2Cu_3O_{6+y}$ (YBCO) compound, as discovered in 1987 by Wu and co-workers, is the first material that became superconducting at boiling nitrogen temperature. The material contains three copper-oxide layers in a unit cell: two of them — CuO_2 planes — are separated by yttrium atom, the third — basal plane (CuO_y), is surrounded by two barium atoms. The oxygen can be introduced into the basal plane and its content can be varied from 6 to 7 per formula ($0 \leq y \leq 1$) [1]. As the oxygen content increases (starting from $y = 0$), additional atoms enter basal planes and occupy oxygen sites randomly up to a critical doping, for which tetragonal-orthorhombic (T-O) phase transition occurs. For higher dopings oxygen in basal planes becomes partially ordered (for the maximum oxygen content $y = 1$ it becomes fully ordered in chains). The oxygen in the basal

plane acts as a charge reservoir introducing holes into CuO_2 plane copper atoms. However, charge concentration can be also changed by substituting yttrium atoms with calcium [2].

The temperature-doping phase diagram of YBCO contains a characteristic and well-known double plateau feature (60 K and 90 K). While the latter is believed to be optimum with a very small overdoped region, the origin of the former one is still under discussion. Some authors suggest it could be explained by ordering of the oxygen atoms within basal planes [3–6], the other underline its possible purely electronic nature: superconductivity is weakened at the carrier concentration of 1/8 which results in emergence of the plateau [7]. Our goal is to create a semi--microscopic model of YBCO and consistently study the influence of two factors that can contribute to the existence of the plateau: oxygen ordering within chains and doping imbalance between chains and copper-oxide layers. As in Ref. [8], we perform "reverse engineering" approach, i.e. we try to find values of the model parameters that reproduce experimentally observed $T_c(y)$ dependence. In both cases it is possible to obtain the experimental phase diagram, however only in the latter it can be done for physically reasonable values of model parameters. Thus, we use this fact to reject the first of the factors as unimportant for the existence of the 60 K plateau.

2. Model

In underdoped high-temperature superconductors, two temperature scales of short-length pairing correlations and long-range superconducting order seem to be well separated [9]. We consider the situation, in which local superconducting pair correlations are established and the relevant degrees of freedom are represented by phase factors $0 \leq \varphi_\ell(\boldsymbol{r}_i) < 2\pi$ placed in a lattice with nearest neighbor interactions ($\boldsymbol{r}_i$ numbers lattice sites within ℓ-th ab plane). The system becomes superconducting while the U(1) symmetry of the $\varphi_\ell(\boldsymbol{r}_i)$ factors is spontaneously broken and the non-zero value of $\langle \mathrm{e}^{\mathrm{i}\varphi_\ell(\boldsymbol{r}_i)} \rangle$ appears signaling the long-range phase order. The Hamiltonian that we consider consists of four parts

$$H[\varphi] = H_\parallel + H_\perp + H'_\parallel + H'_\perp \tag{1}$$

containing various microscopic phase stiffnesses representing characteristic energy scales present in YBCO:

1. in-plane coupling $J_\parallel > 0$ within CuO_2 layers

$$H_\parallel = -J_\parallel \sum_\ell \sum_{i<j} [\cos(\varphi_{3\ell}(\boldsymbol{r}_i) - \varphi_{3\ell}(\boldsymbol{r}_j)) + \cos(\varphi_{3\ell+1}(\boldsymbol{r}_i) - \varphi_{3\ell+1}(\boldsymbol{r}_j))]; \tag{2}$$

2. inter-plane coupling $J_\perp > 0$ between neighboring CuO_2 layer

$$H_\perp = -J_\perp \sum_\ell \sum_{i<j} \cos(\varphi_{3\ell}(\boldsymbol{r}_i) - \varphi_{3\ell+1}(\boldsymbol{r}_i)); \tag{3}$$

3. in-plane coupling $J'_{\parallel} > 0$ within basal planes, which can be gradually turned off along a direction by anisotropy parameter $\eta \in [0,1]$ to simulate oxygen ordering along b direction

$$H'_{\parallel} = -J'_{\parallel} \sum_{\ell} \sum_{i} \sum_{j=-1,1} [\cos(\varphi_{3\ell+2}(\boldsymbol{r}_i) - \varphi_{3\ell+2}(\boldsymbol{r}_i + j\hat{b})) + \eta \cos(\varphi_{3\ell+2}(\boldsymbol{r}_i) - \varphi_{3\ell+2}(\boldsymbol{r}_i + j\hat{a}))]; \tag{4}$$

4. inter-plane coupling $J'_{\perp} > 0$ between adjacent CuO_2 layer and basal plane

$$H'_{\perp} = -J'_{\perp} \sum_{\ell} \sum_{i<j} [\cos(\varphi_{3\ell+1}(\boldsymbol{r}_i) - \varphi_{3\ell+2}(\boldsymbol{r}_i)) + \cos(\varphi_{3\ell+2}(\boldsymbol{r}_i) - \varphi_{3\ell+3}(\boldsymbol{r}_i))]. \tag{5}$$

The indices i, j go from 1 to $N_{\parallel}$ being the number of sites in a plane, $\ell = 1, \ldots, N_{\perp}/3$, where $N_{\perp}$ denotes the number of layers and $N = N_{\parallel} N_{\perp}$ is the total number of sites. The partition function of the system is simply

$$Z = \int_0^{2\pi} \prod_{\ell,i} \mathrm{d}\varphi_{\ell}(\boldsymbol{r}_i) \mathrm{e}^{-\beta H[\varphi]}, \tag{6}$$

where $\beta = 1/k_{\mathrm{B}}T$ and T is temperature. It is more convenient to write the Hamiltonian in a vector form. Thus, we introduce two-dimensional vectors $\boldsymbol{S}_{\ell}(\boldsymbol{r}_i) = [S_{x\ell}(\boldsymbol{r}_i), S_{y\ell}(\boldsymbol{r}_i)]$ of the unit length $\boldsymbol{S}^2_{\ell}(\boldsymbol{r}_i) = S^2_{x\ell}(\boldsymbol{r}_i) + S^2_{y\ell}(\boldsymbol{r}_i) = 1$ defined by $\boldsymbol{S}_{\ell}(\boldsymbol{r}_i) = [\cos\varphi_{\ell}(\boldsymbol{r}_i), \sin\varphi_{\ell}(\boldsymbol{r}_i)]$. The Hamiltonian reads then

$$Z = \int_0^{2\pi} \Big[\prod_{\ell,i} \mathrm{d}^2 \boldsymbol{S}_{\ell}(\boldsymbol{r}_i) \delta(\boldsymbol{S}^2_{\ell}(\boldsymbol{r}_i) - 1) \Big] \mathrm{e}^{-\beta H[S]}, \tag{7}$$

where the unit length constraint ($\boldsymbol{S}^2_{\ell}(\boldsymbol{r}_i) = 1$) is introduced by the set of Dirac-δ functions. Since the partition function in Eq. (6) cannot be calculated exactly it is necessary to replace the rigid length constraint in Eq. (7) by a weaker spherical closure relation

$$\delta(\boldsymbol{S}^2_{\ell}(\boldsymbol{r}_i) - 1) \to \delta \left(\frac{1}{N} \sum_{i,\ell} \boldsymbol{S}^2_{\ell}(\boldsymbol{r}_i) - 1 \right). \tag{8}$$

Furthermore, the introduction of different microscopic phase stiffnesses for CuO_2 and basal planes breaks translational symmetry along c axis (the inter-plane and in-plane couplings vary with period of 3). Since, in such situation, a standard way of diagonalizing the Hamiltonian using three-dimensional Fourier transform of variables ($\boldsymbol{S}_{\ell}(\boldsymbol{r}_i)$ in this case) fails, we implement a combination of two-dimensional Fourier transform for in-plane vector variables

$$\boldsymbol{S}_{\ell}(\boldsymbol{r}_i) = \frac{1}{N_{\parallel}} \sum_{\boldsymbol{k}} \boldsymbol{S}_{\boldsymbol{k}\ell} \mathrm{e}^{-\mathrm{i}\boldsymbol{k}\boldsymbol{r}_i} \tag{9}$$

and transfer matrix method for one-dimensional decorated structure along c-axis [10]. This former operation diagonalizes all terms in the Hamiltonian in Eq. (1) with respect to $\boldsymbol{k}$, leaving the dependence on layer index ℓ unchanged.

Therefore, the partition function can be written in the form

$$Z = \int_{-\infty}^{+\infty} \frac{\mathrm{d}\lambda}{2\pi\mathrm{i}} \exp\Big(N\lambda + \ln \int_{-\infty}^{+\infty} \prod_{\boldsymbol{k},\ell} \mathrm{d}^2 \boldsymbol{S}_{\boldsymbol{k}\ell} \times \exp\big(-\frac{1}{N_\parallel} \sum_{\boldsymbol{k},\ell,\ell'} \boldsymbol{S}_{\boldsymbol{k}\ell} A^{\ell\ell'}_{N_\perp}(\boldsymbol{k}) \boldsymbol{S}_{-\boldsymbol{k}\ell'}\big)\Big), \tag{10}$$

where $A^{\ell\ell'}_{N_\perp}(\boldsymbol{k})$ is an element of a square $N_\perp \times N_\perp$ band matrix, appearing as a result of non-trivial coupling structure along c-direction. The problem reduces then to the evaluation of a determinant of the $A^{\ell\ell'}_{N_\perp}(\boldsymbol{k})$ matrix (for technical details, we refer readers to Refs. [8, 11]). Finally, we arrive at the expression for the critical temperature

$$\beta_\mathrm{c} = \frac{2}{3} \int_{-1}^{+1} \mathrm{d}\xi \int_{-1}^{+1} \frac{\mathrm{d}\zeta \rho(\xi)\rho(\zeta)[2J'^2_\perp + J^2_\perp - 4\alpha(\alpha + 2\alpha')]}{\sqrt{\big[(J'^2_\perp - 2\alpha\alpha')^2 - (J_\perp\alpha')^2\big]\big[(2\alpha)^2 - J^2_\perp\big]}}, \tag{11}$$

where $\alpha \equiv \lambda_0/\beta - J_\parallel(\xi + \zeta)$, $\alpha' \equiv \lambda_0/\beta - J'_\parallel(\xi + \eta\zeta)$ and $\rho(\varepsilon)$ is a density of states of the chain (one-dimensional) lattice given by

$$\rho(\varepsilon) = \frac{1}{\pi} \frac{1}{\sqrt{1 - \varepsilon^2}} \Theta(1 - |\varepsilon|), \tag{12}$$

$\Theta(x)$ is the unit-step function, and λ is a Lagrange multiplier introduced by representing the Dirac-δ function in a spectral form $\delta(x) = \int_{-\infty}^{+\infty} \mathrm{d}\lambda/(2\pi\mathrm{i}) \exp(-\lambda x)$.

3. Oxygen ordering and the critical temperature

The result of Eq. (11) provides us with a tool to analyze the influence of anisotropy and characteristic energy scales present in YBCO at the critical temperature. However, in order to describe YBCO phase diagram, it is necessary to relate the model parameters to the amount of oxygen doping. Therefore, we are using a phenomenological dependence of in-plane microscopic phase stiffness of CuO_2 plane on charge (hole) concentration, which was successfully used to describe properties of superconducting homologous series [8]. Furthermore, the dependence between charge concentration and oxygen amount in YBCO was determined experimentally by Tallon et al. and found out to be roughly linear in the superconducting region (charge concentration changes from $\delta = 0.05$ for $y = 0.4$ to $\delta = 0.17$ for $y = 1$) [12]. Consequently, the in-plane phase stiffness as a function of oxygen amount reads $J_\parallel(y) = J_\parallel g(y)$, where

$$J_\parallel(y) = J_\parallel \times \begin{cases} 1 - \frac{1}{0.55^2}(y - 0.95)^2 & \text{for} \quad 0.4 \le y \le 1, \\ 0 & \text{for} \quad y \le 0.4. \end{cases} \tag{13}$$

Since the T-O phase transition and emergence of superconductivity in YBCO do not occur for exactly the same doping [13], we suggest the following scenario describing the phase diagram of YBCO: while increasing oxygen doping (starting from $y = 0$), the onset of superconductivity is reached ($y = 0.4$). The critical temperature is rising up to a point, in which T-O phase transition occurs ($y = 0.5$). For higher dopings, oxygen chains start to form. As a result, the chain layers

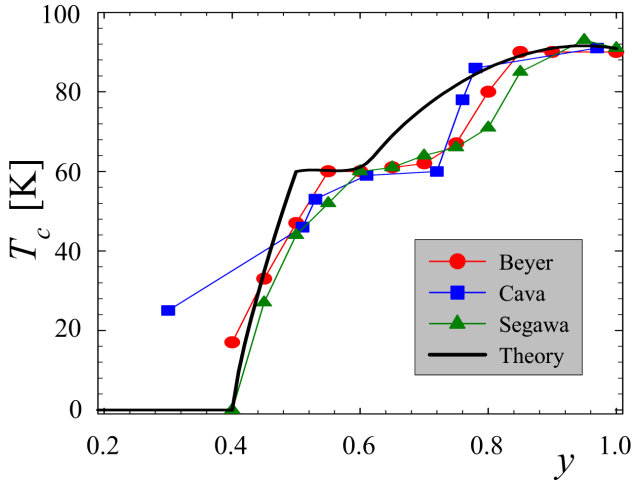

Fig. 1. Comparison of experimental phase diagrams of YBCO (from Refs. [14, 15, 7]) with results of the presented model.

become quasi one-dimensional, which increases the phase fluctuations. Since this factor acts destructively on the phase ordering, the critical temperature is constant in spite of the doping being increased. Further, while all the oxygen is ordered in chains, the critical temperature roughly follows in-plane phase stiffness $J_{\parallel}$ dependence on doping reaching its maximum value of 93 K for $y = 0.95$ and dropping slightly later. In order to confirm this scenario we need to calculate the values of model parameters $J_{\parallel}$, $J'_{\parallel}$, $J_{\perp}$, $J'_{\perp}$ and the doping dependence of anisotropy parameter $\eta(\delta)$ which would reproduce an experimental phase diagram. Utilizing experimental data from penetration depth experiments and the fact that temperatures of YBCO plateaus are 60 K and 90 K we find the needed values: $J_{\parallel} = 19.32$ meV, $J'_{\parallel} = 33.81$ meV, $J_{\perp} = J'_{\perp} = 0.58$ meV while

$$\eta(\delta) = \frac{1}{3}[(2-2\delta)^{15.2} + (2-2\delta)^{7.9} + (2-2\delta)^{3.6}]. \tag{14}$$

The resulting phase diagram predicted by the model along with experimental results is presented in Fig. 1 (thick solid line). It is obvious that the procedure reproduces the characteristic features of YBCO phase diagram: 60 K plateau, 93 K maximum critical temperature with small overdoped region. However, one can notice that the position and size of the 60 K plateau on the phase diagram is a little bit different than the experimental results show. Unfortunately, the value of basal plane in-plane microscopic phase stiffness $J'_{\parallel}$ is almost twice bigger than CuO_2 planes coupling $J_{\parallel}$ which seems to be unphysical. For more reasonable values $J_{\parallel} > J'_{\parallel}$, the influence of anisotropy in basal planes is almost negligible and the experimental phase diagram cannot be reproduced. Thus, we find it rather unlikely that oxygen ordering into chains alone can explain the existence of the 60 K plateau.

4. Charge imbalance and the critical temperature

YBCO can be doped not only by adding the oxygen atoms, but also by substituting three-valent yttrium atoms with two-valent calciums, which introduces holes directly to CuO_2 planes leaving apical and basal sites untouched (charge is not transferred to the basal sites) [2]. This suggests that charge concentration within apical sites along with basal plane sites and CuO_2 layers can be significantly different. Consequently, one can imagine that an increase in oxygen amounts changes charge concentration primarily in the basal regions and only some of the charges are transported to the copper-oxide layers. In fact, this scenario has been confirmed by means of site-specific X-ray absorption spectroscopy [2]. Because increasing doping of underdoped and overdoped superconductors has the opposite influence on the critical temperature, this may provide two counteracting factors leading to the emergence of the 60 K plateau. To test this scenario within the presented model we allow the doping of copper-oxide layers and apical sites to be different and calculate the actual values that reproduce the experimental $T_c(y)$ dependence. It appears that the dependence can be reproduced perfectly, however, only if in the whole region of oxygen doping in which YBCO is superconducting, basal planes along with apical sites are overdoped while *simultaneously* CuO_2 planes are underdoped. This leads to the following scenario for the YBCO phase diagram (see Fig. 2): for a small oxygen amount, CuO_2 planes and apical sites are underdoped (Fig. 2a). Once both reach the minimal charge concentration of 6% the superconductivity sets in. The critical temperature is rising up to the oxygen amount of about $y = 0.5$, when the apical sites reach the optimal charge concentration. Later on the competition between two counteracting factors (underdoped CuO_2 planes and overdoped apical sites) leads initially to the 60 K plateau and further — to the rise in T_c up to its maximum value (Fig. 2b). Finally, when CuO_2 planes also become overdoped for $y = 0.95$, the critical temperature is reduced slightly toward $y = 1$ (Fig. 2c).

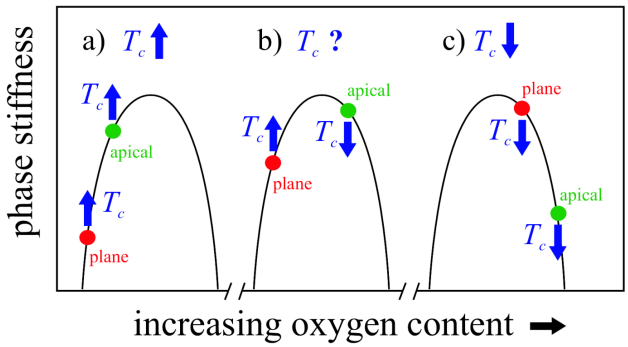

Fig. 2. Change of the critical temperature with oxygen doping of charge imbalanced YBCO: (a) underdoped material, (b) 60 K plateau region, (c) overdoped region.

5. Summary and conclusions

The aim of the present paper was to discuss a possible origin of the 60 K plateau of the YBCO phase diagram. To this end we have proposed a model of $YBa_2Cu_3O_{6+y}$ and analyzed the influence of oxygen ordering and doping imbalance on the shape of the phase diagram. We found out that, although, the shape of the phase diagram can be recreated including the effects of oxygen ordering only, the actual model parameters seem to be unphysical. Therefore, we have rejected this scenario and proposed the other one, based on experimentally observed charge imbalance between CuO_2 planes and CuO chain oxygen sites. We were able to show that the 60 K plateau may be a result of the fact that in an almost whole region in which YBCO is superconducting, copper-oxide layers are underdoped, while oxygen apical sites are overdoped. The competition between two factors of which one tends to increase while the second — to decrease — the critical temperature leads to a non-trivial dependence of T_c on doping, i.e. the 60 K plateau.

References

[1] J.M.S. Skakle, *Mater. Sci. Eng.* **R23**, 1 (1998).

[2] M. Merz, N. Nücker, P. Schweiss, S. Schuppler, C.T. Chen, V. Chakarian, J. Freeland, Y.U. Idzerda, M. Kläser, G. Müller-Vogt, Th. Wolf, *Phys. Rev. Lett.* **80**, 5192 (1998).

[3] A. Ourmazd, J.C.H. Spence, *Nature (London)* **329**, 425 (1987).

[4] C. Chaillout, M.A. Alario-Franco, J.J. Capponi, J. Chenavas, J.L. Hodeau, M. Marezio, *Phys. Rev. B* **36**, 7118 (1987).

[5] H.F. Poulsen, N.H. Andersen, J.V. Andersen, H. Bohrt, O.G. Mouritsen, *Nature (London)* **349**, 594 (1991).

[6] Y. Yan, M.G. Blanchin, C. Picard, P. Gerdanian, *J. Mater. Chem.* **3**, 603 (1993).

[7] K. Segawa, Y. Ando, *J. Low Temp. Phys.* **131**, 822 (2003); M.K. Wu, J.R. Ashburn, C.J. Torng, P.H. Hor, R.L. Meng, L. Gao, Z.J. Huang, Y.Q. Wang, C.W. Chu, *Phys. Rev. Lett.* **58**, 908 (1987).

[8] T.A. Zaleski, T.K. Kopeć, *Phys. Rev. B* **71**, 014519 (2005).

[9] V.J. Emery, S.A. Kivelson, *Nature* **374**, 434 (1995).

[10] S. Fishman, T.A.L. Ziman, *Phys. Rev. B* **26**, 1258 (1982).

[11] T.A. Zaleski, T.K. Kopeć, *Phys. Rev. B* **74**, 014504 (2006).

[12] J.L. Tallon, C. Bernhard, H. Shaked, R.L. Hitterman, J.D. Jorgensen, *Phys. Rev. B* **51**, 12911 (1995).

[13] L. Li, S. Cao, F. Liu, W. Li, C. Chi, C. Jing, J. Zhan, *Physica C* **418**, 43 (2005).

[14] R. Beyers, B.T. Ahn, G. Gorman, V.Y. Lee, S.S.P. Parkin, M.L. Ramirez, K.P. Roche, J.E. Vazquez, T.M. Gür, R.A. Huggins, *Nature (London)* **340**, 619 (1989).

[15] R.J. Cava, B. Batlogg, C.H. Chen, E.A. Rietman, S.M. Zahurak, D. Werder, *Nature (London)* **329**, 423 (1987).